

## VERY LOW ENERGY SUPERNOVAE FROM NEUTRINO MASS LOSS

ELIZABETH LOVEGROVE<sup>1</sup> AND S. E. WOOSLEY<sup>1</sup>

*Draft version September 7, 2021*

### ABSTRACT

The continuing difficulty of achieving a reliable explosion in simulations of core-collapse supernovae, especially for more massive stars, has led to speculation concerning the observable transients that might be produced if such a supernova fails. Even if a prompt outgoing shock fails to form in a collapsing presupernova star, one must still consider the hydrodynamic response of the star to the abrupt loss of mass via neutrinos as the core forms a protoneutron star. Following a suggestion by Nadezhin (1980), we calculate the hydrodynamical responses of typical supernova progenitor stars to the rapid loss of approximately 0.2 to 0.5  $M_{\odot}$  of gravitational mass from their centers. In a red supergiant star, a very weak supernova with total kinetic energy  $\sim 10^{47}$  erg results. The binding energy of a large fraction of the hydrogen envelope before the explosion is of the same order and, depending upon assumptions regarding the neutrino loss rates, most of it is ejected. Ejection speeds are  $\sim 100$  km s<sup>-1</sup> and luminosities  $\sim 10^{39}$  erg s<sup>-1</sup> are maintained for about a year. A significant part of the energy comes from the recombination of hydrogen. The color of the explosion is extremely red and the events bear some similarity to “luminous red novae,” but have much lower speeds.

*Subject headings:* black holes - supernovae: general, stars:neutron, neutrinos, shock waves

### 1. INTRODUCTION

Black holes are expected to form in a significant fraction of massive star deaths (e.g., O’Connor & Ott 2011; Ugliano et al. 2012) and it seems possible that in at least some of these cases the black hole will form without generating an outgoing shock. What observable signal would accompany such an event? Would they all be “un-novae” (Kochanek et al. 2008), stars that just disappear from view, or will some sort of transient display announce the birth of any black hole?

If the progenitor star was rotating, then a variety of energetic transients might be possible depending on the distribution of angular momentum, ranging from common gamma-ray bursts by the collapsar mechanism (Woosley 1993; MacFadyen & Woosley 1999) to long duration x-ray (MacFadyen et al. 2001; Li 2003) and gamma-ray (Quataert & Shiode 2012; Woosley & Heger 2011) transients. But what if the star were rotating very slowly or not at all? Pulsations (Woosley & Heger 2007) or acoustic energy transport (Quataert & Shiode 2012) may lead to envelope ejection, but these either occur in stars that are uncommonly massive or depend on details of gravity wave propagation that are still to be worked out.

Here we follow on a suggestion by Nadezhin (1980) which provides a simple mechanism for ejecting at least some mass in supernova progenitors with very weakly bound envelopes, i.e., red supergiants. In all but extremely rare super-massive stars, iron core collapse leads to protoneutron star formation (O’Connor & Ott 2011). The protoneutron star must then emit a considerable fraction of its mass-energy as neutrinos before either settling down as a cold degenerate object or contracting inside its event horizon and becoming a black hole. This is true even if the protoneutron star continues to accrete substantial mass while contracting. In fact, in that case,

the total energy emitted should be close to the binding energy of a neutron star with its maximum stable gravitational mass, which we allow to vary in the range 2.0 - 2.5  $M_{\odot}$  in our model.

As frequently noted, this huge energy loss also results in a decrease in the gravitational mass of the compact object (Lattimer & Yahil 1989; Lattimer & Prakash 2001). This mass loss is of order

$$BE \approx 0.084 \left( \frac{M_G}{M_{\odot}} \right)^2 M_{\odot} \quad (1)$$

where  $M_G$  is the gravitational mass of the cold neutron star. This implies a mass loss of approximately 0.2 - 0.5  $M_{\odot}$  over a period of several seconds, far shorter than the sound crossing time for the helium and heavy element core. This “mass” streams out through the presupernova star at the speed of light without interacting appreciably. To the remaining star it simply appears that the gravitational potential of the core has abruptly decreased. In response, the star begins to expand. In this paper we simulate this mass loss and the resulting expansion to determine whether it is capable of creating a shock with sufficient energy to reach the outer layers of the star and, if it does, to eject mass and form a visible transient. It is important to note that this expansion precedes the loss in support pressure caused by the collapse of the core. That rarefaction passes out through the star on a slower, free-fall time scale.

### 2. COMPUTATIONAL PROCEDURE

We began with two presupernova models calculated using the KEPLER stellar evolution code. KEPLER is a Lagrangian 1D implicit hydrodynamics code with the appropriate nuclear physics, mass loss, opacities, and equations of state for studying massive star evolution (Weaver et al. 1978; Woosley et al. 2002). It is not Courant-limited, allowing it to follow a star from its formation to the collapse of its iron core. How-

<sup>1</sup>Department of Astronomy and Astrophysics, University of California, Santa Cruz, CA 95064; woosley@ucolick.org

ever, because KEPLER uses a Lagrangian grid, it cannot easily implement an absorbing inner boundary condition. Consequently, it cannot accurately follow the infall of the star once a compact object has formed at its center. Once the presupernova models calculated by KEPLER reached supersonic collapse speeds in their cores, they were thus mapped into CASTRO<sup>2</sup> for further study. CASTRO is a multidimensional Eulerian radiation-hydrodynamics code with adaptive mesh refinement, stellar equations of state, nuclear reaction networks and self-gravity (Almgren 2010). The calculations were done in one dimension with reactions turned off, and the central object modeled as a point of variable mass. An Eulerian grid with constant mesh and spherical geometry was employed. After the collapse had proceeded long enough in CASTRO to allow shock propagation to the base of the hydrogen envelope, the results were then mapped back into KEPLER again and the final hydrodynamics and a light curve were calculated.

### 2.1. Central Object Modeling

Hydrodynamics and radiation transport in the region immediately surrounding a protoneutron star or black hole is complex and difficult to model. A realistic simulation of the neutrino transport alone is well beyond the scope of this paper and the outcome would depend upon the chosen neutron star equation of state and the dimensionality of the calculation. Since we are only interested in the temporal evolution of the central gravitational potential, however, reasonably good results can be obtained from parametrized calculations with a generic, qualitative description of the neutrino energy loss. The inner boundary of our simulation is placed, in CASTRO, at the outer edge of the pre-collapse iron core. Matter interior to this boundary is treated as a point having variable gravitational mass. Initially this mass is equal to the baryonic mass of the interior matter, i.e., the iron core mass. As time passes that gravitational mass decreases due to neutrino emission and, if no mass were added, it would eventually decrease to the known cold neutron star value for a given baryonic mass and equation of state (Prakash et al. 1997). However, appreciable mass does accrete, leading in the more interesting cases to the formation of a black hole. During the accretion phase neutrinos continue to carry away effective mass. Since we neglect rotation, we assume that, after the black hole forms, matter and energy flow into the black hole without any more emission.

An upper limit to the mass lost is given by the gravitational binding energy of the maximum stable neutron star mass, the ‘‘Tolman-Oppenheimer-Volkoff (TOV) limit’’ (Oppenheimer & Volkoff 1939). Current best limits place this parameter in the range 2.0 to 2.5  $M_{\odot}$  of gravitational mass (Akmal et al. 1998; Demorest et al. 2010). The characteristic time scale for this loss, which is assumed to occur exponentially, is given by the cooling timescale parameter  $\tau_c$ , taken here to be 3 seconds (e.g. Burrows & Lattimer 1987). For this simple case, the mass loss rate is

$$\dot{M}_G = \frac{BE}{\tau_c} e^{-t/\tau_c} \quad (2)$$

<sup>2</sup> Code version as of May 2012.

This equation gives an upper bound on the mass loss and therefore on the strength of the transient produced. This model is referred to as the ‘‘maximum mass loss’’ case.

Somewhat more realistically, we can take into account the time for the critical mass to accrete and follow the neutrino energy losses that occur during that time. For each bit of mass that accretes, some fraction of its gravitational binding energy is radiated away promptly, but more is emitted with a delay since the neutrinos must diffuse out. Once the black hole has formed, the neutrino-emitting material falls within the event horizon much faster than the neutrino diffusion timescale, and any energy that has not been released by the time of collapse ends up in the black hole (Prakash et al. 1997; Burrows 1988). The protoneutron star is also extremely hot and thus behaves in a slightly different manner from cold neutron stars. We represent the protoneutron star as a low-entropy core surrounded by a hot envelope and track three masses:  $M_{Gh}$ ,  $M_B$ , and  $M_{th}$ .

$M_B$  is the baryonic mass, i.e. all mass that either was inside the inner boundary at the time of collapse or subsequently accretes through the inner boundary.  $M_{Gh}$  is the effective gravitational mass of the hot neutron star, which is *not*, in general, equivalent to  $M_o$ , the gravitational mass of a *cold* neutron star with the same baryon content. This is the mass that defines the gravitational potential in the outer part of the star.  $M_{th}$  accounts for the difference in mass-energy stored in this hot neutron star as opposed to a cold one, due to both its higher internal energy and inflated radius. This extra internal energy diffuses away on the cooling timescale  $\tau_c$ . The gravitational mass  $M_{Gh}$  of the hot neutron star is then:

$$M_{Gh} = M_o + M_{th} \quad (3)$$

$$= M_B - BE_c + M_{th} \quad (4)$$

where  $BE_c$  is the cold neutron star binding energy. As matter accretes a fraction  $\epsilon$  of the subsequent change in binding energy is assumed to be trapped and added to  $M_{th}$  while the remaining fraction  $1 - \epsilon$  is radiated promptly as neutrinos. The trapped energy diffuses out on a cooling timescale  $\tau_c$ . The evolution of  $M_{th}$  is thus given by

$$\dot{M}_{th} = -\frac{M_{th}}{\tau_c} + \epsilon \frac{dBE_c}{dM_B} \dot{M}_B \quad (5)$$

and the initial condition  $M_{th} = BE_c$ . The derivative  $dBE_c/dM_B$  is evaluated from the binding energy equation, Eq. 1. Once all  $M_{th}$  has diffused away, i.e. the neutron star has cooled, Eq. 4 reduces to the standard cold neutron star equation  $M_G = M_B - BE_c$ . Assuming rapid virialization of the accreted material implies that the parameter  $\epsilon$  should not exceed  $\sim 0.5$ . As the cooling timescale at the surface is likely less than the timescale for the full PNS,  $\epsilon$  is likely to be much lower. In the limit that the cooling timescale were much shorter than the accretion timescale,  $\epsilon$  would go effectively to zero. For our models we adopt  $\epsilon = 0.1$ . In Section 3.3 we test the effects of varying this parameter and find them to be small.

The emission halts when the neutron star has accreted past the TOV maximum mass limit. However this limiting mass must be adjusted for the neutron star’s evolving heat content. Therefore we wait until the cold core of the neutron star ( $M_{Gh} - M_{th}$ ) has accreted past the

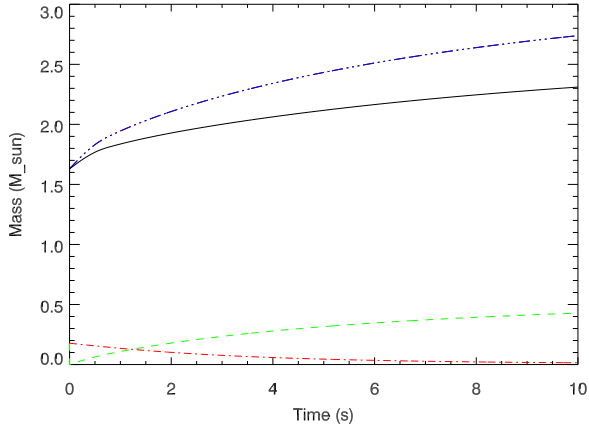


FIG. 1.— Core mass growth in the  $15 M_{\odot}$  model RSG15 with an assumed TOV mass limit of  $2.5 M_{\odot}$ , demonstrating the “full loss” model. The black curve (solid) shows  $M_{Gh}$ , the gravitational mass. Blue (dash-triple dot) is  $M_B$ , the baryonic mass. Red (dash-dot) is the thermal mass  $M_{th}$ . Green (dashed) shows the cumulative lost mass from the simulation.

TOV limit before we assume the core has become a black hole and shut off the neutrino emission. From this point on the central object behaves as a purely gravitational point mass that absorbs all of  $\dot{M}_B$ . This is referred to as the “full loss” model.

Figure 1 shows an example of the full model for RSG15, TOV =  $2.5 M_{\odot}$ . The blue curve shows  $M_B$ , the total baryonic mass that has entered the core region (pre-collapse core plus accretion); it is higher than the black curve showing  $M_{Gh}$ , the effective gravitational mass of the core. The red curve shows  $M_{th}$ , which decays exponentially as the proton-neutron star cools. The green curve shows the cumulative mass loss in the simulation. Even though the core in this case lives for almost 24 s as a neutron star, most of the mass loss occurs during the first 5 seconds.

## 2.2. Choice and Structure of Stellar Models

The two presupernova models used for this paper were red supergiants with a ZAMS mass of  $15 M_{\odot}$  (RSG15), shown in Fig. 2, and  $25 M_{\odot}$  (RSG25), shown in Fig. 3, both of solar metallicity. They are taken from the survey of Woosley & Heger (2007). Both stars shed substantial amounts of mass before reaching the end of their lives. The  $15 M_{\odot}$  star represents a more common supernova progenitor, while the  $25 M_{\odot}$  model has a more compact structure and may be more likely to make a black hole promptly. The observed upper limit on the progenitor masses of standard core-collapse supernovae found to date is  $18 M_{\odot}$  (e.g. Smartt 2009), suggesting that higher mass progenitors are more likely to collapse in a non-traditional way, or that these progenitors are preferentially obscured. Model RSG15 has a helium core of  $4.27 M_{\odot}$  that extends to  $3.568 \times 10^{10}$  cm. RSG25 has a helium core of  $8.20 M_{\odot}$  that extends to  $1.807 \times 10^{10}$  cm. Both red supergiants have an extended, tenuously-bound hydrogen envelope extending from the helium core out to  $\sim 5 \times 10^{13}$  cm that is easily ejected. The net binding energy of the envelope external to what is nominally the helium core (where the hydrogen mass fraction declines to 1%) is  $1.1 \times 10^{48}$  erg, but a short distance out at  $4.48 M_{\odot}$  this declines to  $10^{47}$  erg, a value that character-

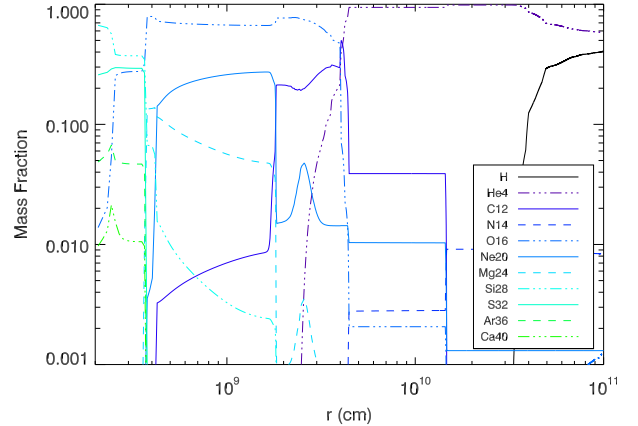


FIG. 2.— Composition of the RSG15 supernova progenitor star.

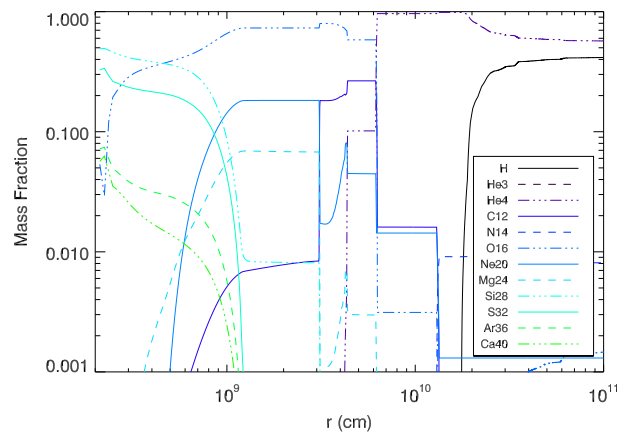


FIG. 3.— Composition of the RSG25 supernova progenitor star.

izes most of the hydrogen envelope. These values include internal energy but not the energy potentially available from recombination. For the  $25 M_{\odot}$  model, the net binding energy external to the helium core is  $6.4 \times 10^{48}$  erg, but this declines to  $10^{47}$  erg when the interior mass increases from  $8.20 M_{\odot}$  to  $8.36 M_{\odot}$  and a still smaller value characterizes most of the envelope. We note that the recombination of  $10 M_{\odot}$  of hydrogen (13.6 eV per atom) would release  $2.6 \times 10^{47}$  erg.

Some additional parameters of both models can be found in Table 1. Also given is the compactness parameter,  $\xi_{2.5}$ , as defined by O’Connor & Ott (2011), but computed at the time when the star is moved to CASTRO rather than at the time of core bounce. A star with a higher compactness parameter has a denser region surrounding its core; for our purposes, this means it will accrete to the TOV limit faster and therefore potentially lose less mass as neutrinos.

Because of the extended size of the red supergiant progenitors, we do not carry the entire star on our simulation grid in CASTRO. Instead we model only the helium core and base of the hydrogen envelope.

## 3. HYDRODYNAMIC RESPONSE

### 3.1. Models Without Mass Loss

Without an outgoing shock or mass loss from neutrinos, the inner layers of the star should collapse directly into the black hole. This scenario provides an excellent

TABLE 1  
STELLAR MODEL PARAMETERS

Model Name	Final Mass ( $M_{\odot}$ )	He Core Mass ( $M_{\odot}$ )	He Core Radius (cm)	Compactness $\xi_{2.5}$
RSG15	12.79	4.27	$3.568 \times 10^{10}$	0.18
RSG25	15.84	8.20	$1.807 \times 10^{10}$	0.33

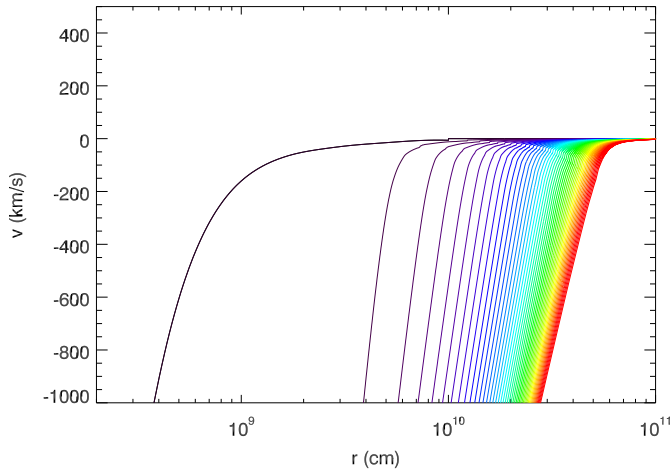


FIG. 4.— Velocity curves showing collapse of the RSG15 stellar model in the prompt black hole formation case, i.e. without any mass loss. Positive velocities are outwards, negative are inwards. Curves are purple for early times, shading to red for late, approximately 15 s spacing. With no mass decrement and no core bounce shock to provide outward velocity, the star simply falls into the black hole. Total time shown: 709 s.

check of the fidelity of our simulation. As Figure 4 shows, our model accurately reproduces this behavior. Dark (purple) colors on the plot indicate early times, shading to light (red) colors at late times. Initially the bulk of the star is in hydrostatic equilibrium (zero velocity) with a small portion near the core showing high infall velocities. As the collapse continues, more and more of the stellar material acquires negative velocities. Without an outgoing shock to counter this motion, it eventually falls into the core. If the simulation is run for long enough, all mass will disappear from the grid. Physically, this scenario corresponds to prompt black hole formation, when the core collapses without passing through an intermediate protoneutron star stage. If the outer layers of the star do not have sufficient angular momentum to form a disk when they reach the black hole, the entire star will disappear without producing a transient - the unnova case as defined by Kochanek et al. (2008).

Figure 5 shows the growth of the simulated point mass in RSG15. The black curves show the model with no neutrino mass loss; in this case the point mass corresponds to  $M_B$ . The dashed line represents the growth of the point mass while the dot-dashed line shows the mass on the simulated grid. Over time this point mass grows as the grid mass declines, with most of the change occurring in the first 15 seconds. The solid line shows the sum of the point mass and grid mass, i.e. the total mass represented in the simulation; in the no-mass-loss case it is constant throughout. This confirms that our simulation is reproducing the collapse accurately, without spurious shocks or unphysical mass loss.

### 3.2. Models With Maximum Mass Loss

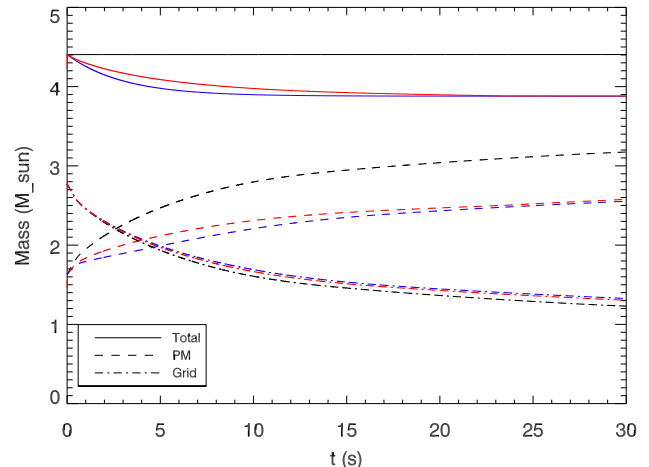


FIG. 5.— Various core masses as a function of time for Model RSG15 and a TOV limit of  $2.5 M_{\odot}$ . The central mass  $M_{Gh}$  (dashed) grows while the mass on the simulation grid (dot-dashed) drops. The solid line represents the total mass in the center and on the grid combined. Black curves show the no neutrino loss (constant mass) case. Blue curves show the maximum-loss model, while the red curves show the full neutrino loss model.

The set of blue curves in Figure 5 shows the evolution using the simplified maximum mass loss model. In this case, the point mass corresponds to  $M_G$  with losses defined by Eq. 2, in which the core loses the total binding energy appropriate to a TOV-limit neutron star on a time scale  $\tau_c$ , regardless of the amount of mass flowing in from the collapsing star. This model therefore provides an upper bound on possible transients, as the core cannot lose more mass than the binding energy of the largest possible neutron star. The amount of mass lost in each case is listed in Table 2. Following the blue curves in Figure 5, as the collapse begins the point mass growth (dashed) is noticeably suppressed for the first 5 seconds as neutrino losses balance accreted mass. The overall mass in the simulation (solid) drops accordingly, then becomes constant as mass loss ceases.

This mass decrement was sufficient to produce an outgoing shock in the inner layers of the  $15 M_{\odot}$  presupernova star. The shock's evolution is seen in Figure 6 (purple at early times, shading to red at late times). The shock grows in speed as it leaves the helium core, and succeeds in reaching the base of the hydrogen envelope. Of interest is the fact that the shock strength varied noticeably with the choice of neutron star upper mass limit. The approximate shock strengths at  $10^{11}$  cm for our six different choices of TOV limit are listed in Table 2.

### 3.3. Models With Realistic Neutrino Mass Loss

The red curves in Figure 5 show the mass evolution for the full model for neutrino losses described in Section 2.1. In this case the dashed line showing the point mass

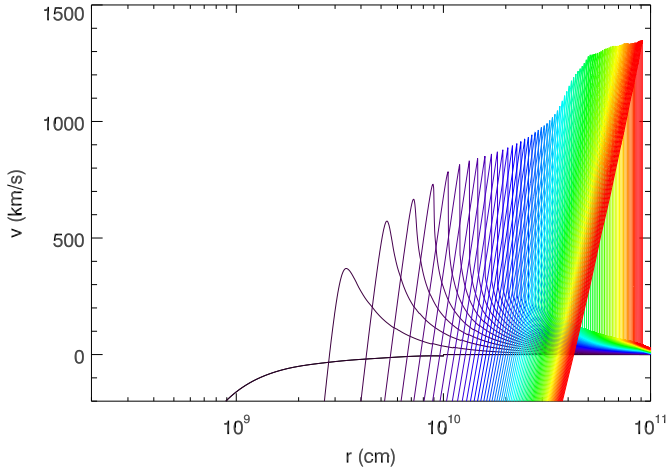


FIG. 6.— Collapse of the RSG15 model in the maximum neutrino mass loss case, showing a shock forming due to the effective core mass decrement. Positive velocities are outwards, negative are inwards. Curves are purple for early times, shading to red for late. This model has the TOV limit set to 2.5, resulting in a mass decrement of  $0.525 M_{\odot}$ . The shock propagates out of the helium core ( $r = 3.568 \times 10^{10}$  cm). Time shock reaches  $10^{10}$  cm: 38 s. Time to end of helium core: 196 s. Time to  $10^{11}$  cm: 577 s.

corresponds to  $M_{Gh}$  as given by Eq. 4. This model takes into account the thermal mass loss and ties the cessation of neutrino losses to the amount of material that has been accreted by the core, rather than switching it off after a predetermined timescale as in the upper bound model. As can be seen in Figure 5, this model (red) loses mass over a longer timescale than the maximum loss model (blue), continuing until the point mass reaches the TOV limit, in this case  $2.5 M_{\odot}$ , after which the total mass becomes constant. We expect equal or less mass loss in this case as compared to the maximum loss model. In the case where the TOV limit is high enough that the neutron star lives for longer than the cooling timescale, the core loses close to the maximum possible amount of mass; in the case where it does not, however, mass loss is suppressed as neutrinos that would have been emitted instead end up inside the black hole. The amount of mass lost in each case is listed in Table 3.

Though the overall mass decrement in the full model cases is lower than in the maximum loss case, it is still sufficient to produce an outgoing shock. Figure 7 shows the shock evolution for RSG15, TOV =  $2.5 M_{\odot}$ . The approximate shock strengths at  $10^{11}$  cm for our six different choices of TOV limit are listed in Table 3. The six shocks created in RSG15 are shown in Figure 8.

We also tested variations in the parameter  $\epsilon$ , which controls the fraction of binding energy trapped as thermal mass. Changes in  $\epsilon$  have a small but real effect on the total mass loss, depending on the amount of accreted mass. The more mass accreted, the more important  $\epsilon$  will be. As higher TOV limit models tend to accrete longer,  $\epsilon$  has a higher impact here. A lower epsilon leads to a higher mass loss as less of the binding energy is temporarily trapped as thermal mass. We tested the range  $\epsilon < 0.5$ , identified as the physically reasonable range of this parameter. For the case where the TOV limit is  $2.5 M_{\odot}$ , the most sensitive, a change of 0.05 in  $\epsilon$  in RSG25 resulted in approximately a  $0.011 M_{\odot}$  change in the overall mass loss. In the extreme case  $\epsilon = 0.5$ , this will make

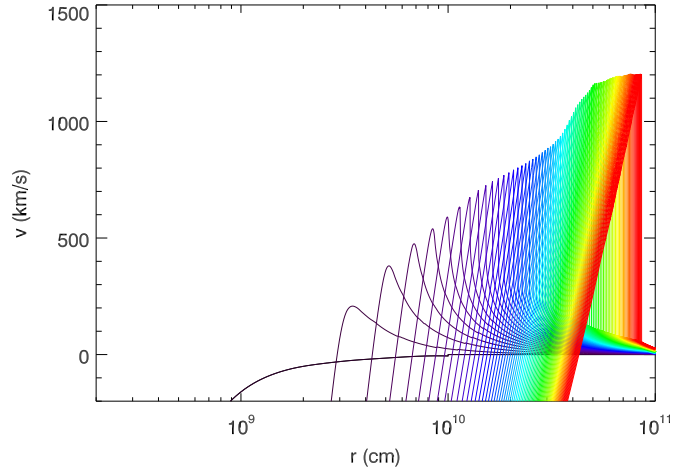


FIG. 7.— Collapse of the RSG15 model in the fully-modeled neutrino mass loss case, showing a shock forming due to the effective core mass decrement. Positive velocities are outwards, negative are inwards. Curves are purple for early times, shading to red for late. This model has the TOV limit set to 2.5, resulting in a mass decrement of  $0.523 M_{\odot}$ . The shock is smaller in strength than the maximum-loss case and reaches the edge of the simulation with a lower velocity. Time shock reaches  $10^{10}$  cm: 40 s. Time to end of helium core: 207 s. Time to  $10^{11}$  cm: 620 s.

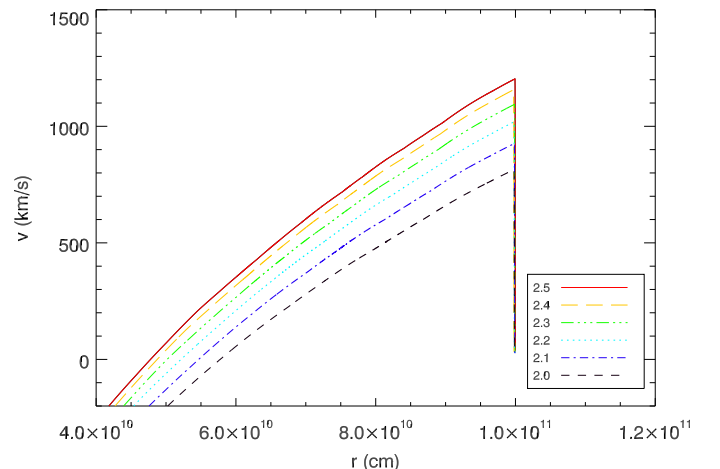


FIG. 8.— RSG15 shocks at the limit of the CASTRO simulated domain for six different choices of TOV limit, full neutrino loss model.

a TOV =  $2.5 M_{\odot}$  model look like a TOV  $\sim 2.35 M_{\odot}$  model. For lower TOV limits, the effect of varying  $\epsilon$  was smaller. Thus, although a change in  $\epsilon$  will affect the mass decrement and by extension the shock strength, the results are robust.

### 3.4. Effects of Stellar Structure

The kinetic energy of the shock that reaches the hydrogen envelope is strongly influenced by the size of the presupernova core and the overlying stellar structure through which it must travel, as can be seen by the differences in kinetic energy between RSG25 and RSG15 in the maximum mass loss model. This model loses the same amount of mass in the same time regardless of stellar structure, but the final shock in RSG25 models is significantly weaker than in RSG15, having propagated through a much heavier carbon-oxygen and helium core

TABLE 2  
MAXIMUM MASS LOSS MODELS

Stellar Model	TOV ( $M_{\odot}$ )	Mass Lost ( $M_{\odot}$ )	KE <sup>a</sup> (ergs)	Shock Strength <sup>b</sup> (km/s)
RSG15	2.0	0.336	$1.875 \times 10^{47}$	902
...	2.1	0.370	$2.599 \times 10^{47}$	985
...	2.2	0.407	$3.572 \times 10^{47}$	1070
...	2.3	0.444	$4.855 \times 10^{47}$	1158
...	2.4	0.484	$6.554 \times 10^{47}$	1249
...	2.5	0.525	$8.719 \times 10^{47}$	1341
RSG25	2.0	0.336	$6.537 \times 10^{46}$	723
...	2.1	0.370	$1.002 \times 10^{47}$	820
...	2.2	0.407	$1.483 \times 10^{47}$	919
...	2.3	0.444	$2.139 \times 10^{47}$	1025
...	2.4	0.484	$3.011 \times 10^{47}$	1134
...	2.5	0.525	$4.148 \times 10^{47}$	1246

<sup>a</sup> At base of hydrogen envelope

<sup>b</sup> At  $r = 10^{11}$  cm

TABLE 3  
FULL MASS LOSS MODELS

Stellar Model	TOV ( $M_{\odot}$ )	Mass Lost ( $M_{\odot}$ )	KE <sup>a</sup> (ergs)	Shock Strength <sup>b</sup> (km/s)
RSG15	2.0	0.277	$1.287 \times 10^{47}$	814
...	2.1	0.331	$2.059 \times 10^{47}$	926
...	2.2	0.382	$2.953 \times 10^{47}$	1019
...	2.3	0.430	$3.911 \times 10^{47}$	1094
...	2.4	0.477	$4.896 \times 10^{47}$	1157
...	2.5	0.523	$5.779 \times 10^{47}$	1204
RSG25	2.0	0.179	$8.418 \times 10^{45}$	394
...	2.1	0.230	$2.893 \times 10^{46}$	569
...	2.2	0.281	$6.581 \times 10^{46}$	725
...	2.3	0.331	$1.204 \times 10^{47}$	866
...	2.4	0.382	$1.930 \times 10^{47}$	996
...	2.5	0.433	$2.827 \times 10^{47}$	1114

<sup>a</sup> At base of hydrogen envelope

<sup>b</sup> At  $r = 10^{11}$  cm

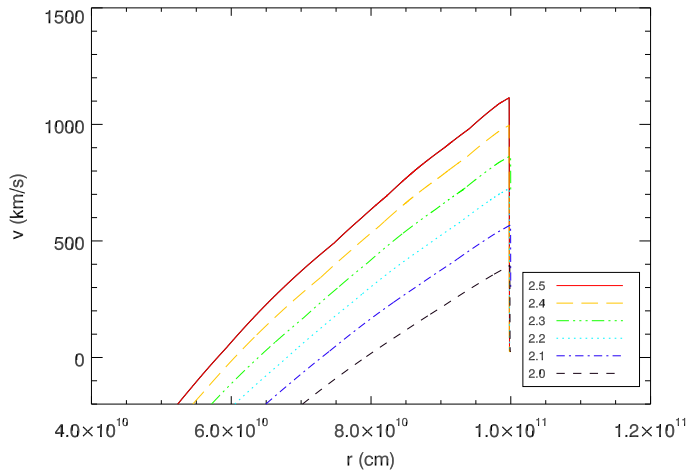


FIG. 9.— RSG25 shocks at the limit of the CASTRO simulated domain for six different choices of TOV limit, full neutrino model. The choice of TOV limit has a stronger effect on the final shock strength in this model than it does in RSG15.

before reaching the hydrogen envelope.

Additional effects come into play when using the full neutrino model based on the speed at which the core accretes. RSG25 has a denser inner structure (higher

compactness) and a more massive iron core of  $1.83 M_{\odot}$ , compared to  $1.63 M_{\odot}$ . As it therefore accretes faster than RSG15 and is already closer to the TOV limit, the core spends significantly less time in the protoneutron star state; consequently the same choice of parameters in the larger star causes less mass loss. The full mass loss model in RSG25 also shows systematically lower mass decrements than the maximum mass loss model in all cases, indicating that even with a high TOV limit and a relatively long-lived protoneutron star, not all the binding energy is being emitted before collapse to a black hole. The six shocks produced in RSG25 are shown in Figure 9.

#### 4. TRANSIENTS PRODUCED

In the case of prompt black hole formation in a star without a high- $J$  outer layer, there is no shock and no visible transient - the star simply disappears. Here we consider further the case of protoneutron star formation and delayed collapse, in which an outgoing shock has formed. Will a detectable transient be produced, intermediate between a complete disappearance and a traditional explosion, as raised by Kochanek et al. (2008)? To evaluate this question we took models from CASTRO where the shock had reached  $1 \times 10^{11}$  cm (the limit of the simulation) and mapped them back into KEPLER,



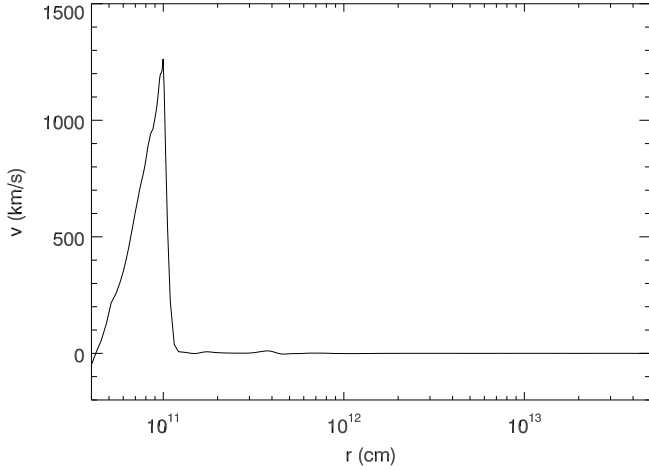


FIG. 10.— Shock modeled by CASTRO in RSG15 (TOV = 2.5, full neutrino losses) mapped into KEPLER.

then continued to evolve them. Figures 10 and 11 show the KEPLER results for RSG15, TOV = 2.5; Figure 10 shows the imported shock, and Figure 11 shows the final velocity of the hydrogen envelope at  $t = 5 \times 10^7$  s.

The shock has decreased significantly in strength by the time it reaches the base of the hydrogen envelope; however, this envelope is very tenuously bound in both RSG15 and RSG25. For each model we tested six choices of TOV limit (2.0 - 2.5  $M_{\odot}$ , in 0.1  $M_{\odot}$  increments) and evaluated the strength of the shock that reached the hydrogen envelope. Using the full neutrino loss model, we found in every case tested for RSG15 and in 3 of 6 tested for RSG25 that the shock produced was larger than  $1 \times 10^{47}$  ergs, the approximate binding energy of the envelope (see Table 3). We can therefore realistically expect the envelope to be ejected in these cases. However, the highest kinetic energy achieved was only of the order of  $6 \times 10^{47}$  ergs, and most models fell well below that number. The envelope is therefore ejected with a very low velocity (50 - 100 km/s). It emits most of its energy via hydrogen recombination. Optically this transient has a low luminosity  $\sim 10^{39} - 10^{40}$  ergs/s, but maintains this luminosity for of order a year. The color temperature of the transient is very red, of order 3000 K. An example light curve can be seen in Figure 12 for RSG15, TOV = 2.5.

The transients calculated here are obviously much fainter and less energetic than standard core-collapse supernova, but they do bear some similarity to a class of recently-observed transients: the “luminous red novae,” such as V838 Mon (Munari 2002). Luminous red novae are too bright to be ordinary classical novae, but too faint and red to be supernovae. Although V838 Mon is now suspected to be a stellar merger event (Tylenda 2011), these two mechanisms have similar end results: a massive hydrogen envelope ejected at low energies. Spectroscopic observations show however that these phenomena have dispersion velocities significantly higher than calculated here. The observation of further transients may decide this question, or a search for remnants. The shedding of a common envelope by a binary merger would leave behind a degenerate remnant, but a failed core-collapse

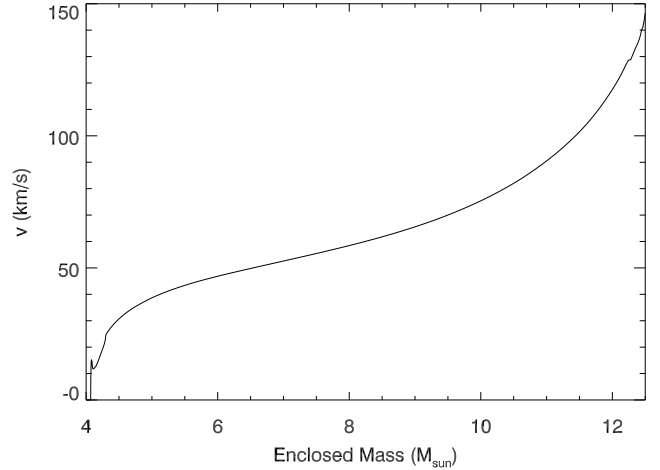


FIG. 11.— Velocity of the hydrogen envelope at  $5 \times 10^7$  s after core collapse in RSG15, TOV = 2.5, full neutrino loss model, evolved further in KEPLER.

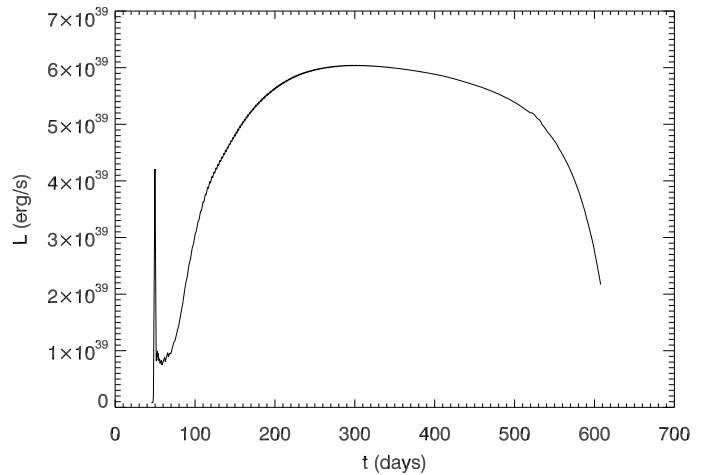


FIG. 12.— KEPLER light curve for a transient from RSG15, TOV = 2.5. The transient is low luminosity but lasts for around a year.

explosion would leave a black hole. A survey such as that proposed by Kochanek et al. (2008), monitoring red supergiants for anomalous transients that might signal the birth of a black hole, should catch these events. They would be visible as a sudden brightening of the “star” for of order a year, followed by a gradual but complete disappearance.

In RSG25 a TOV limit of 2.2  $M_{\odot}$  or lower resulted in such weak outgoing shocks that they could not be accurately followed using KEPLER, and would probably be unable to eject the envelope. In situations where the envelope is not ejected, there is still the possibility of a transient at late times if the envelope is rotating. As it falls back into the black hole, the massive envelope may create a disk and potentially a long-duration gamma-ray transient as described by Woosley & Heger (2011). Since the most massive stars are the ones more likely to produce black holes quickly, it remains possible to produce these long gamma-ray transients. This type of

transient, while invisible in the optical, could emit low levels of gamma rays for months.

A higher TOV limit in the neutron star EOS will increase the probability of these transients occurring. Holding the TOV limit constant, the final strength of the shock is highest in stars with both smaller initial iron core masses (more time spent as a neutron star) and smaller carbon-oxygen and helium core masses. We might therefore expect the strongest transients to come from the lowest-mass red supergiants that fail to form CCSNe. Nucleosynthetic constraints place a lower limit on the maximum mass star that must explode as a supernova most of the time. Brown & Woosley (2013) sets this limit at between 20 and 25  $M_{\odot}$ . Stars above 20  $M_{\odot}$  become more difficult to explode, as measured by their compactness parameter (O’Connor & Ott 2011), and hence more likely to fail. At the same time, in stars above 25  $M_{\odot}$ , it will become increasingly difficult for the shock to reach the surface. We may therefore expect the progenitors of these transients, if they do occur, to land in the range 20 - 25  $M_{\odot}$ .

For heavier stars that lose their hydrogen envelope and die as WR stars, or for stripped progenitors in binaries, a shock can form and may reach the surface, depending on the size of the remaining helium core. Without a large envelope to eject, the transient will be brief but brighter.

## 5. CONCLUSIONS

We have demonstrated that iron core collapse in a massive star is capable of producing a faint observable transient even if the collapse itself creates no prompt outgoing shock. The mass lost to neutrinos results, in some cases, in unbinding the hydrogen envelope. The amount and history of the neutrino mass loss has a strong effect on the magnitude of the shock produced, as does the structure of the carbon-oxygen and helium cores of the progenitor star. In the two red supergiant models tested, the shock reached the base of the hydrogen envelope in a majority of the models with enough energy to eject it. These unusual transients will appear as low-energy, long-duration, red events as the ejected envelope emits its energy via hydrogen recombination. The ejected envelope has a speed on the order of 50 - 100 km/s and maintains a luminosity  $10^{39} - 10^{40}$  ergs/s for approximately a year.

For a given parametrization of the neutrino losses, the transient produced becomes weaker as the TOV mass limit is reduced and as the mass of the presupernova helium core increases. It therefore remains possible, depending upon the TOV limit assumed, to fail to eject the envelope in more massive stars. If the star in these cases has sufficient angular momentum in its outer layers, it may instead produce long gamma-ray transients as described by Woosley & Heger (2011); otherwise it will disappear as an unnova as described by Kochanek et al. (2008).

## 6. ACKNOWLEDGEMENTS

We thank Luke Roberts for insight and guidance in modeling the neutrino losses from a protoneutron star. We thank Ann Almgren and John Bell for providing the CASTRO code and Shawfeng Dong, Chris Malone, and Haitao Ma for assistance with using it. We thank Chris Kochanek and the referee for providing helpful comments. This research has been supported by the

National Science Foundation (AST 0909129), the NASA Theory Program (NNX09AK36G), the DOE High Energy Physics Program (DE-FC02-09ER41438) and two UC Lab Fees Research Awards (09-IR-07-117968 and 12-LR-237070).



## REFERENCES

- Akmal, A., Pandharipande, V. R., & Ravenhall, D. G. 1998, *Phys. Rev. C*, 58, 1804
- Almgren, A. S. 2010, *ApJ*, 715, 1221
- Brown, J., Woosley, S. E., 2013, arXiv:1302.6973
- Burrows, A., 1988, *ApJ*, 334, 891
- Burrows, A., & Lattimer, J. M. 1987, *ApJ*, 318, L63
- Chevalier, R. A. 1993, *ApJ*, 411, L33
- Demorest, P. B., Pennucci, T., Ransom, S. M., Roberts, M. S. E., & Hessels, J. W. T. 2010, *Nature*, 467, 1081
- Fryer, C. L. 1999, *ApJ*, 522, 413
- Kochanek, C. S., Beacom, J. F., Kistler, M. D., Prieto, J. L., Stanek, K. Z., Thompson, T. A., & Yüksel, H. 2008, *ApJ*, 684, 1336
- Lattimer, J. M., & Yahil, A. 1989, *ApJ*, 340, 426
- Lattimer, J. M., & Prakash, M. 2001, *ApJ*, 550, 426
- Li, X.-D. 2003, *ApJ*, 596, L199
- MacFadyen, A. I., & Woosley, S. E. 1999, *ApJ*, 524, 262
- MacFadyen, A. I., Woosley, S. E., & Heger, A. 2001, *ApJ*, 550, 410
- McKinney, J. C. 2006, *MNRAS*, 368, 1561
- Montero, P. J., Janka, H.-T., & Mueller, E. 2011, arXiv:1108.3090
- Munari, U., 2002, *A&A* 2002, 389, L51
- Nadezhin, D. K. 1980, *Ap&SS*, 69, 115
- O'Connor, E., & Ott, C. D. 2011, *ApJ*, 730, 70
- Oppenheimer, J. R., and Volkoff, G. M. 1939, *Phys. Rev.*, 55, 374
- Quataert, E., & Kasen, D. 2011, submitted to *MNRAS*, *MNRAS*, 419, L1
- Quataert, E., & Shiode, J. 2012, arXiv:1202.5036
- Prakash, M., Bombaci, I., Prakash, M., Ellis, P., Lattimer, J., Knorren, R. 1997, *Phys. Rept.*, 280, 1
- Smartt, S. J. 2009, *ARA&A*, 47, 63
- Tylenda, R., Hajduk, M., Kamiński, T., Udalski, A., Soszyński, I., Szymański, M. K., Kubiak, M., Pietrzyński, G., Poleski, R., Wyrzykowski, P., Ulaczyk, K., 2011, *A&A*, 528, A114
- Ugliano, M., Janka, H.-T., Marek, A., & Arcones, A. 2012, *ApJ*, 757, 69
- Weaver, T. A., Zimmerman, G. B., & Woosley, S. E. 1978, *ApJ*, 225, 1021
- Woosley, S. E. 1993, *ApJ*, 405, 273
- Woosley, S. E., Heger, A., & Weaver, T. A. 2002, *Reviews of Modern Physics*, 74, 1015
- Woosley, S. E., & Heger, A. 2007, *Phys. Rep.*, 442, 269
- Woosley, S. E., & Heger, A. 2011, *ApJ*, 752, 32